STANFORD UNIVERSITY

CENTER FOR SYSTEMS RESEARCH

Final Report

DEVELOP MINIMUM THRUSTOR CONTROL LAWS AND SELECT ORBITS FOR A GEODESY DRAG-FREE SATELLITE

Guidance and Control Laboratory

Principal Investigators

Professor John V. Breakwell
Professor Daniel B. DeBra

submitted to

NASA GODDARD SPACE FLIGHT CENTER
Code 551
Grant NAS 5-21714

FEBRUARY 1974

Final Report

DEVELOP MINIMUM THRUSTOR CONTROL LAWS AND SELECT ORBITS FOR A GEODESY DRAG-FREE SATELLITE

submitted to

GODDARD SPACE FLIGHT CENTER OF THE
NATIONAL AERONAUTICS AND SPACE ADMINISTRATION

by

Guidance and Control Laboratory
STANFORD UNIVERSITY

Principal Investigators

Professor John V. Breakwell
Professor Daniel B. DeBra

1974 February

Final Report

DEVELOP MINIMUM THRUSTOR CONTROL LAWS AND SELECT ORBITS FOR A GEODESY DRAG-FREE SATELLITE

INTRODUCTION

The research proposed in Ref. 1 and subsequently made a part of the Work Statement included two specific areas: Research in control laws for pulse plasma systems, and mission analysis. These are discussed separately below. We have summarized principal results but reference the progress letters [2] for many details. In the discussion of the pulse plasma control laws, we have also included some work that has subsequently been done under Ref. 3.

A. PULSE PLASMA CONTROL LAWS

The original motivation for studying control laws for pulse plasma systems was based on the improved life characteristics possible with pulse plasma jets. These pulse plasma units are relatively massive compared with cold gas thrustors. As a result, therefore, significant mass savings can be achieved by minimizing the number of thrustors. The control laws, therefore, were developed for thrust available from two thrustors only. In a spinning satellite, these thrustors are sufficient to completely control the vehicle as long as the spin rate is sufficiently high for a given level of external disturbance. The thrustors are canted so that a component of each is along the + and - spin axis. The other component of each thrustor acts in the radial direction. It is sufficient to analyze the behavior in the plane of spin assuming a single thrustor. The motion along the spin axis is equivalent to a drag-free control system of the type that was flown on the successful DISCOS in 1972 September.

It became clear that this type of control system would be adaptive to a cold gas system also as it can result in considerable simplification. Perhaps more importantly, by having more than one thrustor in the rotating plane, a completely redundant system can be designed with no penalty in

hardware over what is normally used for three-axis control. We have therefore continued our studies beyond the scope of the present contract with innovation for the cold gas thrust system to improve the reliability of the system design being studied under Ref. 3. The early results that were reported in Progress Letters 4 and 5 [of Ref. 2] form the basis on which the more recent research has been performed.

In summary, we have been working with a control law based on neutralizing the velocity with respect to an inertial reference and providing a small component of velocity which drives the proof mass toward the center of the cavity. This algorithm is based on the fact that action can only be taken when the single thrustor is correctly aligned and typically provides impulses with approximately a one-spin-period frequency.

Figure 1 illustrates the dynamical model of the system in which we have the satellite stably spinning in a locally inertial environment. The motion in the spin (z) direction is assumed uncoupled and controlled. The spin plane body axes $\hat{x}_b$, $\hat{y}_b$ are centered at the satellite mass center (c.m.). Initially the position sensor null is also located here. The control action is applied by a component of force from a jet fixed to the satellite along the $-\hat{x}_b$ direction and directed toward the origin. The position of the proof mass is determined by its measured x_b and y_b offsets. In addition, an auxiliary frame N, $(\hat{x}_n, \hat{y}_n)$, is fixed at the satellite mass center, initially coincident with $\hat{x}_b$, $\hat{y}_b$ at some time t_o and maintaining the same orientation relative to some inertially fixed reference. Because of the symmetry of the dynamical model, we treat the motions of the system as if the satellite mass center were inertially fixed and the control were applied to the proof mass in the $-\hat{x}_b$ direction. The magnitude of the force is of course scaled by the mass involved. Finally, we assume that the velocity of the proof mass relative to the satellite c.m. in the N frame and resolved along the $\hat{x}_b$, $\hat{y}_b$ axes is available from a suitable estimator.

The control force is analyzed using two models. First, the control force $(\underline{\Delta V}_c)$ may be specified proportionally above a particular minimum value (ΔV^m). Also, a pulsed control force is considered in which an integral number of pulses of size ΔV^m may be specified. The applicability of these models is determined by the size of ΔV^m and the disturbance environment.

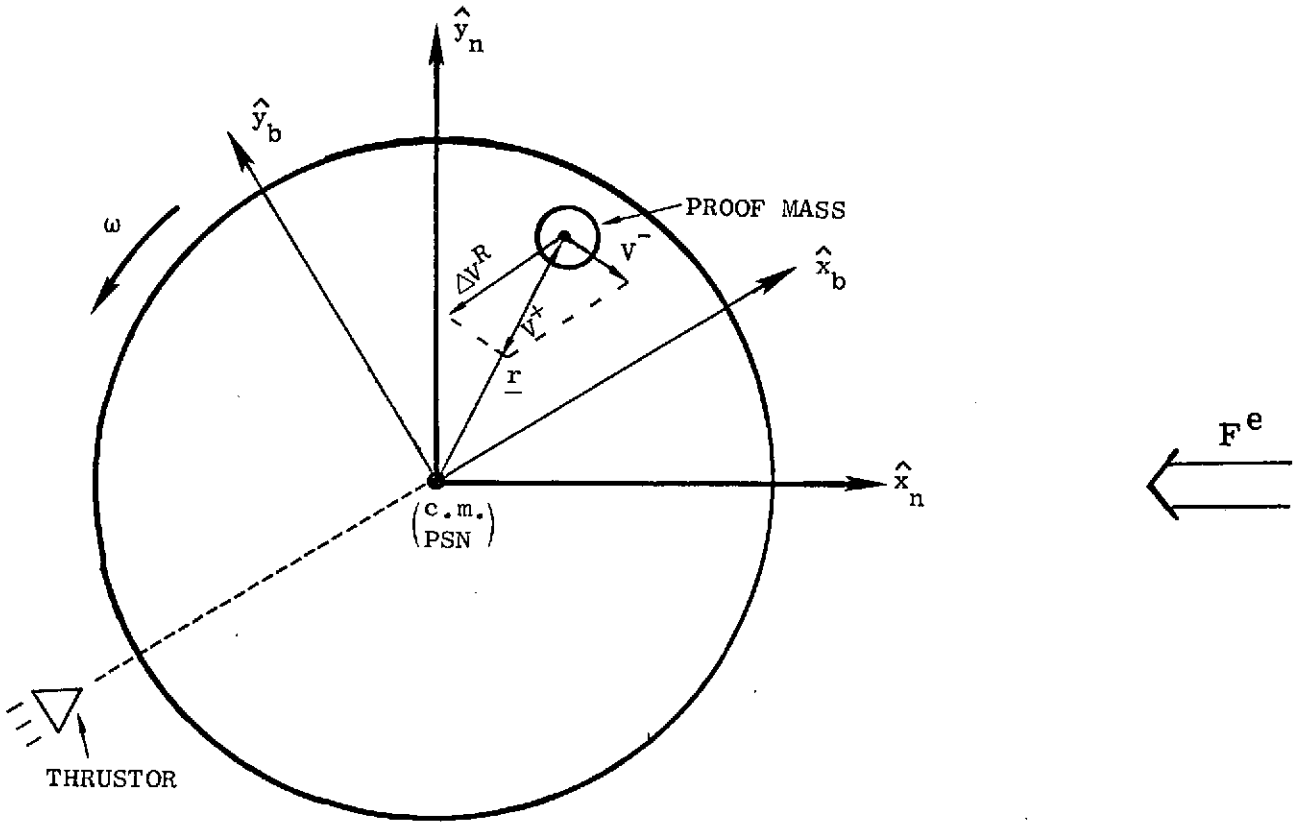

FIGURE 1 AXIS ORIENTATION

Initially, the analysis considers two types of "disturbances". First, an initial proof mass position and velocity is considered. Also, a constant external force (e.g., drag) is assumed in the $-\hat{x}_n$ direction producing a "force" on the proof mass in the $+\hat{x}_n$ direction.

The control logic considered asks that the velocity of the proof mass after control action in the N frame be directed toward the satellite c.m. and be proportional to the distance from the c.m.

Define $\underline{V}^+ \triangleq$ velocity of proof mass in N after control

$\underline{r} \triangleq (x_b, y_b)$ = position vector of proof mass

$\omega \triangleq$ satellite angular rate (constant)

$k \triangleq$ proportionality constant.

Then, the control law would require

$$\underline{V}^+ = -\frac{k}{\pi/\omega}\,\underline{r} \qquad (1)$$

where k measures the fraction of the offset distance travelled by the proof mass in a half satellite revolution. If we define

$\underline{V}^- \triangleq$ velocity of proof mass in N just prior to control

$\underline{\Delta V}^R \triangleq$ required control action

then

$$\underline{\Delta V}^R = -\underline{V}^- - \frac{k}{\pi/\omega}\,\underline{r}\,.$$

Again, defining

$\underline{\Delta V}^A \triangleq$ effect of applied control action on velocity of proof mass,

if we assume the proportional-above-a-minimum control, then from (1):

CL I:
$$|\underline{\Delta V}^A| = \begin{cases} 0, & \underline{\Delta V}^R \cdot \hat{x}_b > 0 \\ 0, & |\underline{\Delta V}^R| < \Delta V^m \quad \underline{\Delta V}^R \cdot \hat{x}_b < 0 \\ |\underline{\Delta V}^R|, & |\underline{\Delta V}^R| > \Delta V^m \quad \underline{\Delta V}^R \cdot \hat{x}_b < 0 \end{cases} .$$

If we assume the integer-pulse control, several logic schemes are available. The first one considered specifies the control applied to be the greatest integer dividend of $|\underline{\Delta V}^A|$ by ΔV^m:

Cl II:
$$|\underline{\Delta V}^A| = \begin{cases} 0 & \underline{\Delta V}^R \cdot \hat{x}_b \geq 0 \\ G\left(\dfrac{|\underline{\Delta V}^R|}{\Delta V^m}\right) \cdot \Delta V^m & \underline{\Delta V}^R \cdot \hat{x}_b < 0 \end{cases}$$

where $G(x/y) \triangleq$ greatest integer dividend of x by y. If we define

$$f = \frac{|\underline{\Delta V}^A|}{\Delta V^m} - G\left(\frac{|\underline{\Delta V}^R|}{\Delta V^m}\right)$$

and assume that f is randomly distributed between 0 and 1, then

$$E(f) = \frac{1}{2} .$$

This average control deficiency manifests itself as a c.m. offset and to compensate for this effect, a third control logic might be specified:

CL III:
$$|\underline{\Delta V}^A| = \begin{cases} 0 & \underline{\Delta V}^R \cdot \hat{x}_b \geq 0 \\ \left[G\left(\dfrac{|\underline{\Delta V}^R|}{\Delta V^m}\right) - \dfrac{1}{2}\right] \cdot \Delta V^m \quad \underline{\Delta V}^R , & \hat{x}_b < 0 \end{cases}$$

In this case $E(f) = 0$ and the average control force is correct.

It was assumed in the analysis that the time history of any control application was much shorter than the spin rate. Thus, the control action consisted of an impulsive ΔV applied of magnitude $|\underline{\Delta V}^A|$. Since the

orientation of the jet is fixed to the body, the direction of $\underline{\Delta V}^A$ is always directed in the $-\hat{x}_b$ direction. Triggering information is derived from the calculation of the component of $\underline{\Delta V}^R$ along the $\hat{y}_b$ axis. When this component is zero, the jet is aligned for firing. The general vector component control logic is as follows:

$$\Delta V^R_{x_b} = \begin{cases} \bar{V}_{x_b} + \frac{k}{\pi/\omega}\, x_b & \Delta V^R_{x_b} > 0 \\ 0 & \Delta V^R_{x_b} \leq 0 \end{cases}$$

$$\Delta V^R_{y_b} = 0$$

$$\Delta V^A_{x_b} = g_{CL}\,(\Delta V^R_{x_b})$$

where g_{CL} is one of the control logic functions specified above.

A hybrid simulation of the plant and controller was assembled on our HP 2114/EAI-TR48 system to determine the performance of the control laws above. Figure 2 depicts this simulation. The dynamics of the proof mass motion were simulated in inertial coordinates, i.e., two uncoupled $1/s^2$ plants. The output was represented by an inertial position and velocity vector

$$\begin{bmatrix} \dot{x}_n \\ \dot{y}_n \end{bmatrix}$$

and

$$\begin{bmatrix} x_n \\ y_n \end{bmatrix}.$$

A rotation vector was generated by an oscillator to produce the driving signal for a coordinate transformation from inertial to body-fixed coordinates, e.g.,

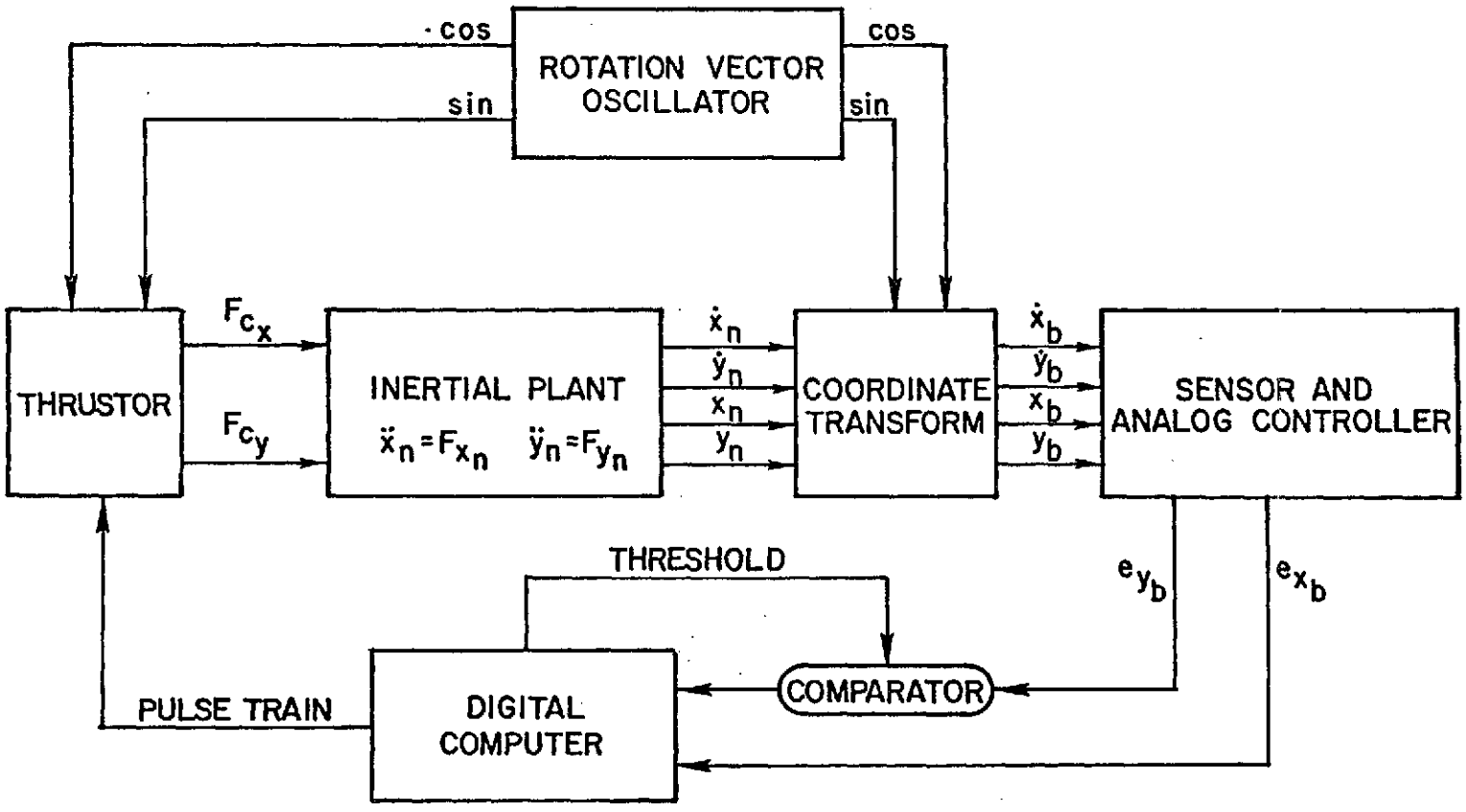

FIG. 2 SINGLE THRUSTOR HYBRID SIMULATION

$$\begin{bmatrix} x_b \\ y_b \end{bmatrix} = \begin{bmatrix} \cos \omega t & \sin \omega t \\ -\sin \omega t & \cos \omega t \end{bmatrix} \begin{bmatrix} x_n \\ y_n \end{bmatrix} .$$

The position and velocity vectors in body coordinates were then input to a sensor model and an analog controller to form the error vector,

$$\begin{bmatrix} e_{x_b} \\ e_{x_b} \end{bmatrix} = \begin{bmatrix} -V_{x_b}^{-} - \frac{k}{\pi/\omega} x_b \\ -V_{y_b}^{-} - \frac{k}{\pi/\omega} y_b \end{bmatrix} ,$$

which corresponds to the required velocity,

$$\begin{bmatrix} e_{x_b} \\ e_{y_b} \end{bmatrix} = \begin{bmatrix} \Delta V_{x_b}^{R} \\ \Delta V_{y_b}^{R} \end{bmatrix} .$$

Thus far the sensor model has been linear with only a null bias offset from the body axis origin (c.m. location).

The e_{yb} signal is compared to a threshold (nominally zero) and a threshold crossing produces a triggering signal to the digital computer. The primary function of the digital computer is to simulate switching control logic. Numerical calculations for the control function are minimal. This is done in consideration for future analog or hard-wired digital circuitry which would be resident in an actual vehicle controller. The

$$e_{x_b} = \Delta V_{x_b}^{R}$$

signal is sensed by the computer and using the control logic (e.g., CLI), the appropriate number of thrustor pulses is calculated. Then a pulse train

is applied to the inertial plant according to a force vector decomposition into inertial coordinates driven by the rotation oscillator

$$\begin{bmatrix} F^C_{x_n} \\ F^C_{y_n} \end{bmatrix} = |\underline{F}^c| \cdot \begin{bmatrix} \cos \omega t \\ \sin \omega t \end{bmatrix}$$

where

$$F^c \triangleq |\underline{F}^c| \hat{x}_b \ ,$$

the control force vector.

A pulsed plasma thrustor with a microsec pulsewidth, 40 μlb-sec impulse size, and 2.5 pulses/sec repetition rate was used as a nominal actuator plant.

Aside from its primary control function, the digital computer was used as a monitoring system for various performance calculations such as fuel consumption and stability. The ability to perform experiments, take data, and calculate results automatically, provide the motivation for the hybrid simulation adopted.

Several qualitative results of the simulation were almost immediately obvious. These are listed below:

1. A finite repetition rate tends to spread the direction of applied force. This effect tends to destabilize the system for large initial conditions and values of k.

2. An adaptive threshold or threshold with memory can stabilize the system for large initial conditions and small repetition rates without a large external force. An external force seems to quickly drive such a system unstable.

3. As $k \rightarrow 1.00$, the system destabilizes in the presence of delays.

4. A dead zone on the position (x_b, y_b) vector tends to drastically reduce the limit cycle size and fuel consumption. It adds stability with long pulse separations. The center of mass (c.m.) hangoff with an external force is not significantly affected.

5. A sensor null bias has a large destabilizing effect. This phenomena is not well understood yet and a stability analysis has been initiated.

6. There is a hangoff of the average proof mass position from the sensor null in the presence of an external force as predicted by the conservation of momentum. The trajectories tend toward one-dimensional as can be seen in Fig. 3. For a smaller external force, the effect is not as pronounced. See Fig. 4.

The fuel consumption of the system was calculated at various values of external force and initial conditions. The results compared quite favorably with the digital computer simulation and are shown in Fig. 5. At higher values of the external force, the number of thrustor firings becomes high and the spreading effect of a finite repetition becomes pronounced. This causes an impulse in the direction transverse to the drag force. This impulse must be taken out if the cross-wise momentum is to be conserved. Using this fact, a correction (to the fuel consumption) for a finite repetition rate can be derived. (see sketch below.)

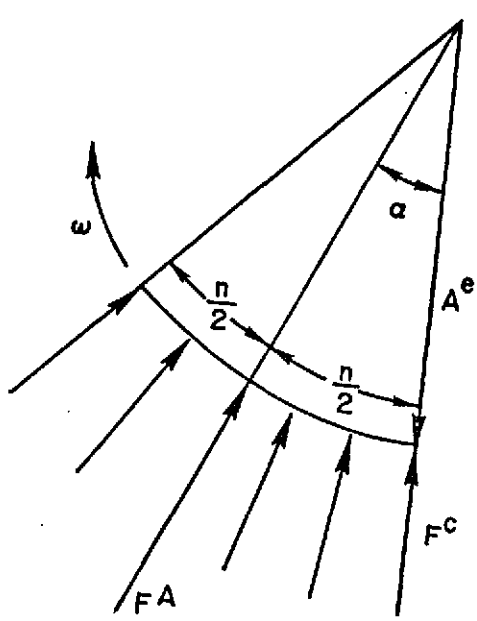

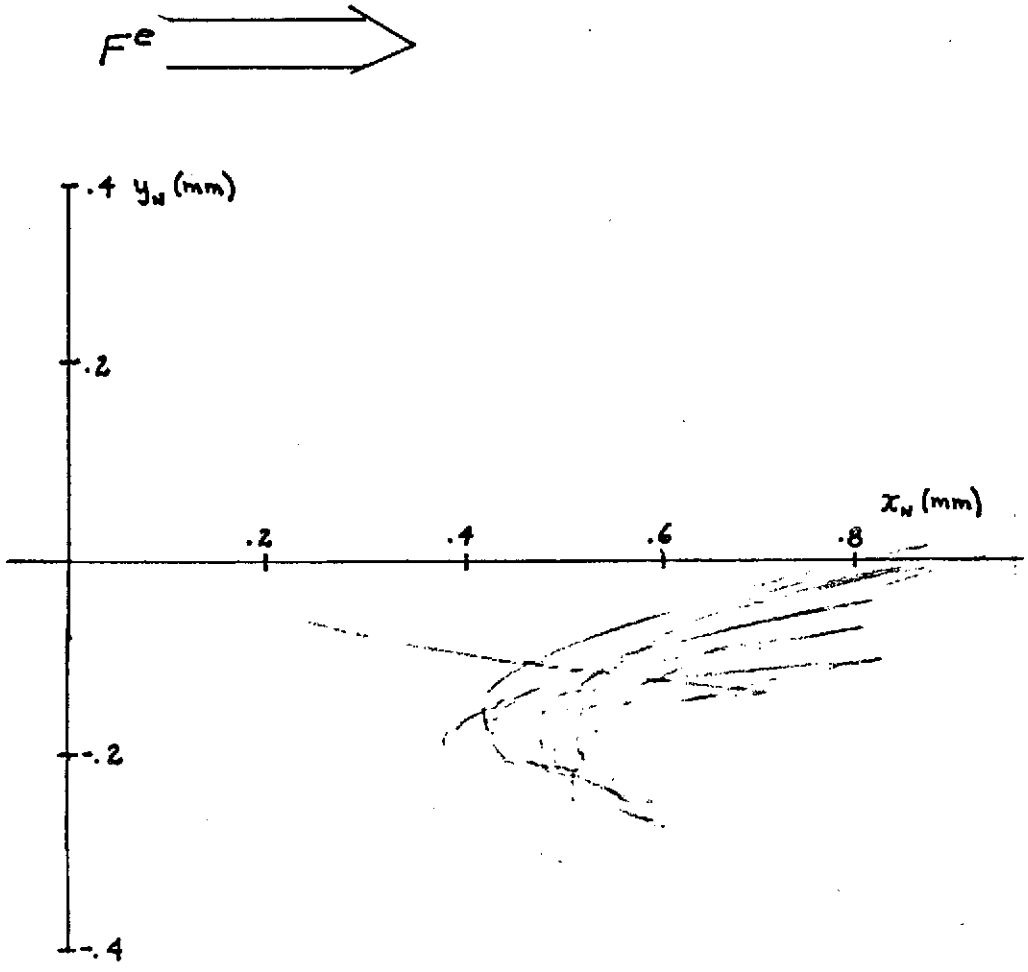

FIG. 3 INERTIAL TRAJECTORIES WITH A LARGE EXTERNAL FORCE.

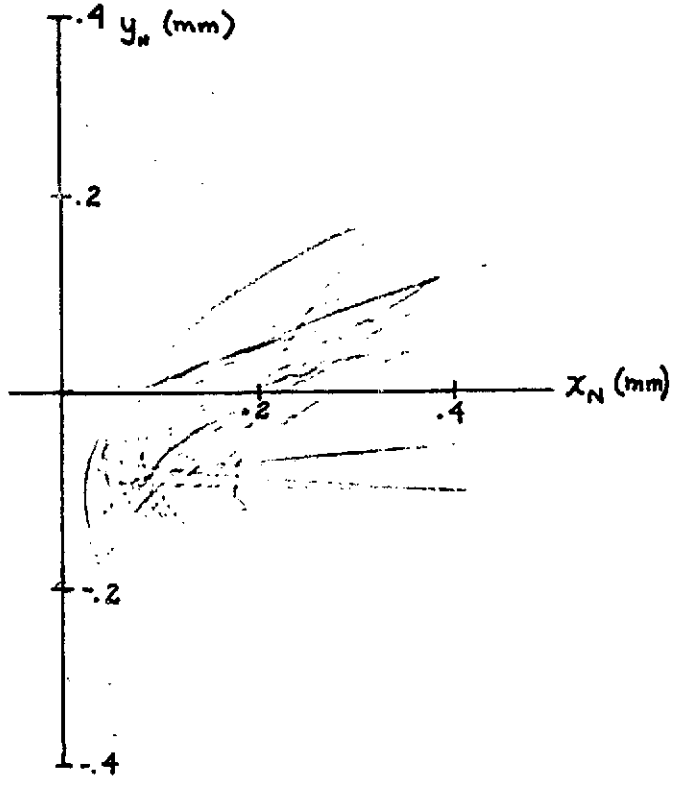

FIG. 4 INERTIAL TRAJECTORIES WITH A SMALL EXTERNAL FORCE.

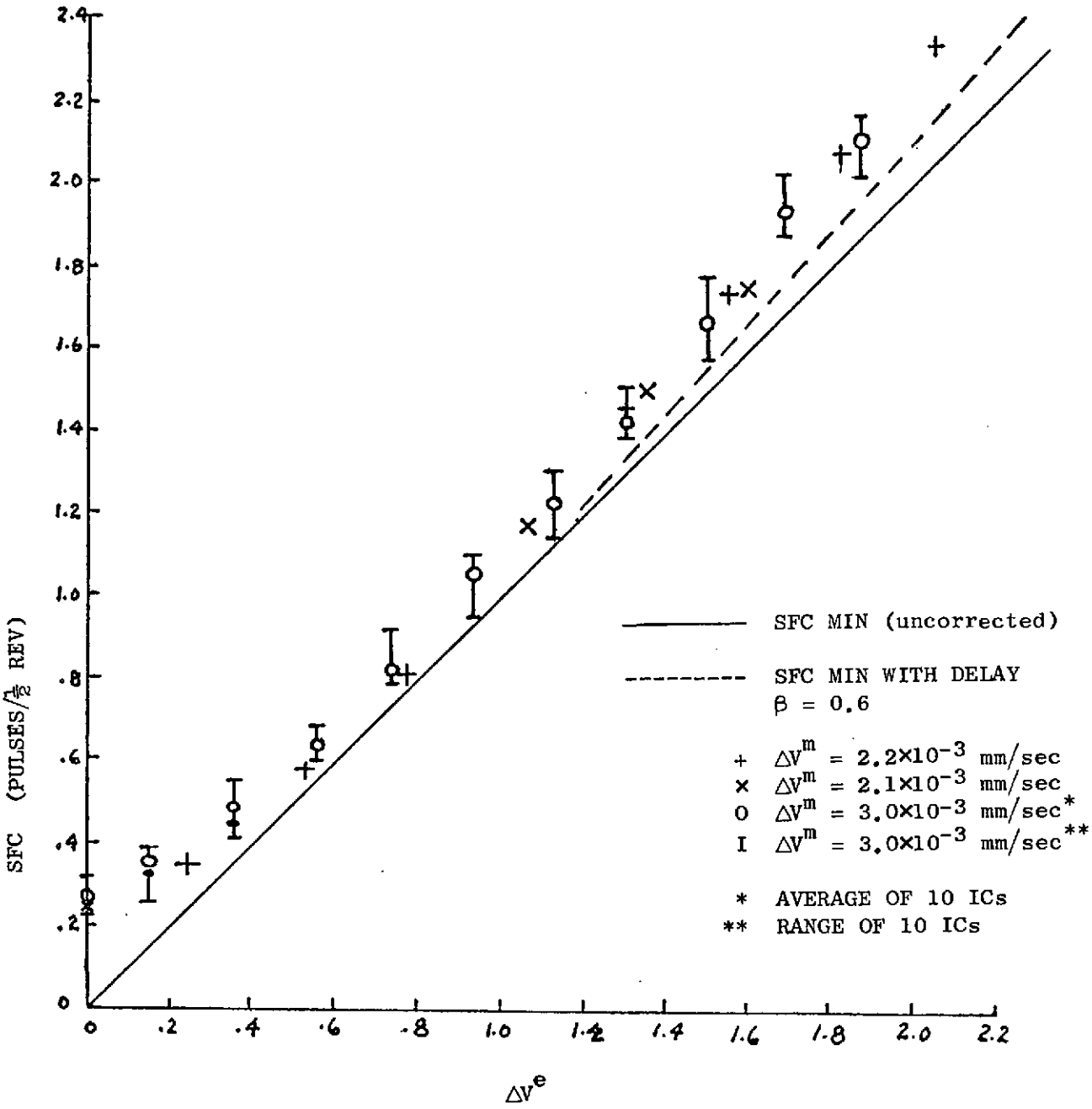

FIG. 5 FUEL CONSUMPTION FOR VARIOUS PULSE WIDTHS SIMULATION RESULTS

Define: $\gamma \triangleq$ repetition rate (pulses/sec)

$\omega \triangleq$ satellite spin rate

$\beta \triangleq \gamma/w$ = rate factor

$F^c \triangleq$ desired control force

$F^A \triangleq$ resultant control force

$\Delta V^T \triangleq$ transverse velocity component

$A^e \triangleq$ external acceleration

$n \triangleq$ number of firings

$\Delta V^m \triangleq$ minimum velocity change (1 impulse) .

Then,

$$\alpha = n/2\beta$$

$$\Delta V^T = n \cdot \Delta V^m \cdot \alpha$$

from intrack conservation of momentum:

$$n \cdot \Delta V^m = A^e \cdot 2\pi/\omega$$

or

$$\Delta V^T = \frac{1}{2}\left(\frac{A^e \cdot 2\pi/\omega}{\Delta V^m}\right)^2 \Delta V^m \cdot \frac{1}{\beta} .$$

But,

$$\frac{\Delta V^T}{2\Delta V^m} = \text{added fuel consumption (pulses/}\tfrac{1}{2}\text{ rev)}$$

$$= 1/\beta(\Delta\tilde{V}^e)^2$$

where

$$\Delta\tilde{V}^e \triangleq A^e{}_T/\Delta V^m .$$

Finally,

$$SFC_{min} = \Delta\tilde{V}^{e} + \frac{1}{\beta}\Delta\tilde{V}^{e^2} \text{ (pulses/}\tfrac{1}{2}\text{ rev)} .$$

These values are shown in Fig. 5 and seem to correlate very well with the simulation results.

We conclude that single thrustor control in the spin plane is (1) stable for the conditions studied, (2) yields fuel consumption approximately equal to the drag except for very low drag levels or spin rates, and (3) is practical to mechanize.

B. MISSION ANALYSIS

INTRODUCTION

Radio altimetry measurement of the ocean surface from a rather low altitude satellite with an accurately known orbit makes it almost mandatory that this orbit be both drag-free and approximately circular. The accurate determination of this low altitude orbit (i.e., determination of the geocentric radius to better than 1 meter) which requires, of course, calibration of tesseral harmonic perturbations which are not accurately known a priori, can be accomplished either with range measurements between a pair of drag-free satellites in the same orbit, or with range measurements from a much higher satellite, possibly also drag-free, on which tesseral perturbations are much smaller and, hopefully, removable.

ANALYTIC DESCRIPTION OF THE LOW ORBIT

This section deals with an analytic description of a near circular, ideally drag-free, orbit. This description is especially suited to the satellite pair ranging method of orbit determination, but it is useful also in the context of orbit determination by range measurements from a high altitude satellite, especially if the high satellite remains in essentially the same plane as the low satellite, e.g., if both orbits are perpendicular to both the equator and the ecliptic planes. The orbit parameters employed are not the conventional ones, but are related to parameters used in earlier research at Stanford University [4, 5]. The effect of tesseral harmonics is described directly in terms of position perturbations rather than orbit element perturbations, and these are expressed in terms of certain coefficients which are combinations of the conventional $C_{\ell m}$, $S_{\ell m}$.

It is assumed that all tesseral resonances (up to fairly high order) are avoided. This assumption about the choice of the low altitude orbit guarantees that no small unknown terms in the expansion of the geopotential can have an unduly large effect on the orbit. An analytic description, which can be good, after fitting, to better than 1 meter is then quite manageable and is represented by the following equations.

$$\frac{r-a}{a} = \frac{\delta r}{a} = -\xi \cos\theta - \eta \sin\theta + \frac{1}{4} J_2 \left(\frac{R_\oplus}{a}\right)^2 \sin^2 i \cos 2\theta + \mathcal{O}_2$$

$$\delta\theta = 2\xi \sin\theta + 2\eta \cos\theta + \frac{1}{8} J_2 \left(\frac{R_\oplus}{a}\right)^2 \sin^2 i \sin 2\theta + \mathcal{O}_2$$

where a is the mean radius (not the average osculating semi-major axis), and (ξ, η) is a "mean eccentricity" vector. Here, θ is a mean orbit position given by

$$\theta = \bar{n}t + \text{constant} ,$$

where $\bar{n}$ (the "nodal mean motion") is given in terms of a by

$$\bar{n} = \left(\frac{\mu_\oplus}{a^3}\right)^{\frac{1}{2}} \left\{1 + J_2 \left(\frac{R_\oplus}{a}\right)^2 \left(\frac{9}{4} - \frac{21}{8} \sin^2 i\right) + \mathcal{O}_2\right\} .$$

It will be useful to assume that i is the inclination of a "best fitting" mean plane regressing at a constant rate $(-\dot{\Omega})$ so that the earth's oblateness gives out-of-plane excursions only of order $J_2\xi$ or $J_2\eta$. This i is not the average osculating inclination. With this definition of the mean plane, out-of-plane excursions are negligible in their contributions to the range between satellites in the same or nearly the same plane. The terms $\mathcal{O}_2$ in the formula for $\bar{n}$ include terms such as J_2^2, J_4, J_6, as well as terms from luni-solar perturbations. All these terms can be obtained from Dasenbrock [4], after finding the relation between the present mean radius a and his parameter $\bar{h}^2/\mu$. The terms $\mathcal{O}_2$ in δr, $\delta\theta$ include terms of second order jointly in J_2, ξ, and η, as well as terms from $J_\ell (\ell \geq 2)$, $C_{\ell m}$, $S_{\ell m}$ $(m \geq 1)$, and from luni-solar perturbations. The tesseral harmonic perturbations may be expressed in the form

$$\frac{1}{a}(\delta r)_{\text{tess.}} = \sum_{\substack{k=-\infty \\ (k,m)\neq(0,0)}}^{\infty} \sum_{m=0}^{\infty} A_{km} \cos(k\theta + m\lambda_N + \phi_{km})$$

$$(\delta\theta)_{\text{tess.}} = \sum_{\substack{k=-\infty \\ (k,m)\neq(0,0)}}^{\infty} \sum_{m=0}^{\infty} B_{km} \cos(k\theta + m\lambda_N + \psi_{km})$$

where λ_N is the longitude of the ascending node, relative to Greenwich.

Here, $$A_{km}\begin{Bmatrix}\cos\\ \sin\end{Bmatrix}\phi_{km} \quad \text{and} \quad B_{km}\begin{Bmatrix}\cos\\ \sin\end{Bmatrix}\psi_{km}$$

are known linear combinations of the usual $C_{\ell m}$, $S_{\ell m}$, with $\ell = |k|, |k| + 2, |k| + 4 \cdots$ [see Morrison, 5].

The mean eccentricity vector (ξ, η) undergoes <u>long period</u> changes:

$$\begin{cases} \frac{d\xi}{d\theta} = -\omega^* \eta + k \\ \frac{d\eta}{d\theta} = \omega^* \xi \end{cases}$$

where

$$\omega^* = J_2\left(\frac{R_\oplus}{a}\right)^2 (2 - \frac{5}{2}\sin^2 i) + \mathcal{O}(J_2^2, J_4, J_6, \cdots) + \text{luni-solar terms}$$

and

k = linear combination of $J_3, J_5, J_7, \cdots$,

all of which are obtainable from Dasenbrock [4].

THE SATELLITE PAIR RANGING METHOD

Figure 6 illustrates the relative geometry of the satellite pair in orbit.

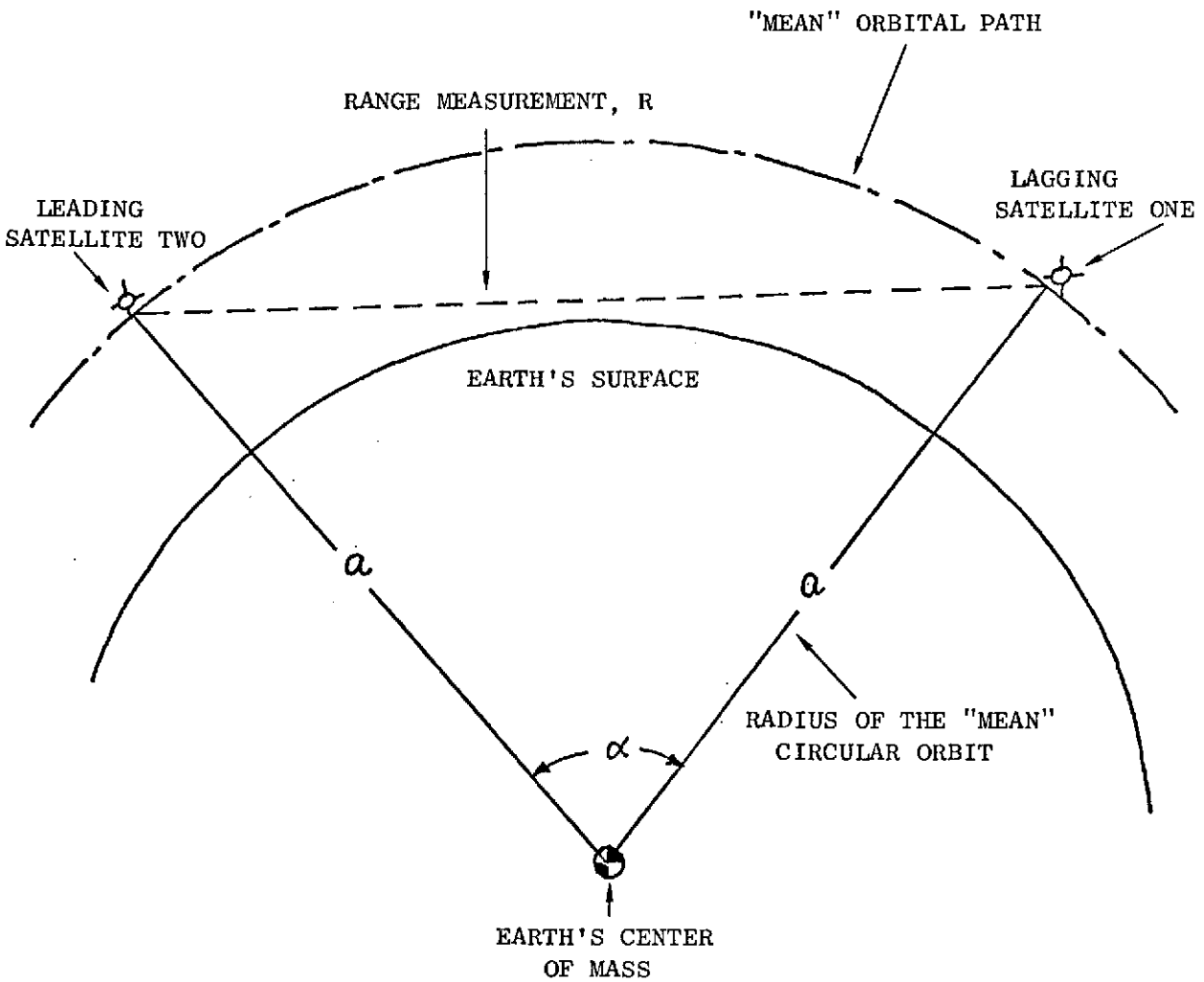

FIG. 6 GEOMETRY OF THE SATELLITE RANGING EXPERIMENT

The fluctuations in the measured range R are expressible as

$$\delta R = (\delta r_1 + \delta r_2) \sin \frac{\alpha}{2} + a(\delta\theta_2 - \delta\theta_1) \cos \frac{\alpha}{2} + \epsilon_2.$$

It is assumed that both satellites are launched together and then drift apart very slowly so that the separation angle α increases from zero up to a maximum permissible separation α_{max}, at which the radio wave passes within 70 km of the earth's surface. For greater separations, the atmospheric refraction will introduce pathlength errors of the order of 1 meter. As soon as α reaches α_{max}, one of the satellites is given a small ΔV either to stabilize α or to reduce it again towards lower values. Prior to reaching α_{max}, the continuous measurement of R provides enough information to determine not only both eccentricity vectors but also all of the coefficients A_{km} and B_{km} up to a high order, with the exception of the coefficients B_{Om} which do not affect R. The ΔV application will introduce a further small change in one of the eccentricity vectors, which, however, is rapidly estimated.

REFINEMENT OF THE EARTH'S GRAVITATIONAL CONSTANT

A side benefit, which is possible from the satellite pair ranging experiment, is the refinement of the earth's gravitational constant $(\mu_\oplus)$, although, as will appear, this refinement improves markedly with an increase in the altitude of the satellite pair.

Present uncertainty in $\mu_\oplus$ is about three parts in 10^6, although tracking data from Mariner 9 may have reduced this uncertainty by a factor of 2. Now the nodal period of the satellite pair is obtainable to very high accuracy from ground tracking. This permits the determination of $\mu_\oplus$ to one part in 10^7 if the mean radius a of either satellite can be determined to better than one part in 3×10^7. It may be assumed that the correction terms in the expression for $\bar{n}$ would be known to better than one part in 10^4 from current values of J_2, J_4 $\cdots$, together with ground tracking determination of i (and a).

To determine a with the required accuracy, consider the measured range with the short period fluctuations averaged out

$$R_{av.} = 2a \sin \frac{\alpha}{2}\left[1 + \mathcal{O}(J_2^2,\ \xi_i^2 + \eta_i^2)\right]$$

where α, the mean separation angle, is expressible as

$$\alpha = \dot{\alpha} t \ .$$

The accuracy with which a itself is estimated depends strongly on the maximum useful α, since for small α, R is essentially the product $(a\dot{\alpha})t$ which is insufficient to estimate a and $\dot{\alpha}$ separately. This accuracy is indicated in Figure 7, showing the bias in estimating a due to a constant bias ΔR in the range measurement, plotted vs useful α.

It has so far been assumed that both satellites are "drag-free", so that the intrack position contains no acceleration due to atmospheric drag. Recent orbital success with a drag-free satellite indicates that the mass attraction of the satellite on the proof mass produces an intrack acceleration of order of magnitude 10^{-11} g. If we assume gravity-gradient stabilized satellites, these accelerations may be assumed essentially constant, but unknown a priori. The estimation of the relative acceleration, together with that of a and $\dot{\alpha}$, slightly degrades the accuracy of the estimate of a (or more correctly, of the mean a during the interval of observation). This is included in Figure 7. However, small fluctuations in the intrack accelerations about their mean values will further degrade the accuracy of estimation of a.

The mean intrack accelerations can be further reduced if the satellites are spun about axes perpendicular to their orbit plane. If the spin period is comparable with the limit-cycle period of the drag-free translation control system, the mass attraction may be expected to fluctuate, but the intrack relative acceleration A should now have essentially zero mean and a fluctuation which may be crudely modeled as a

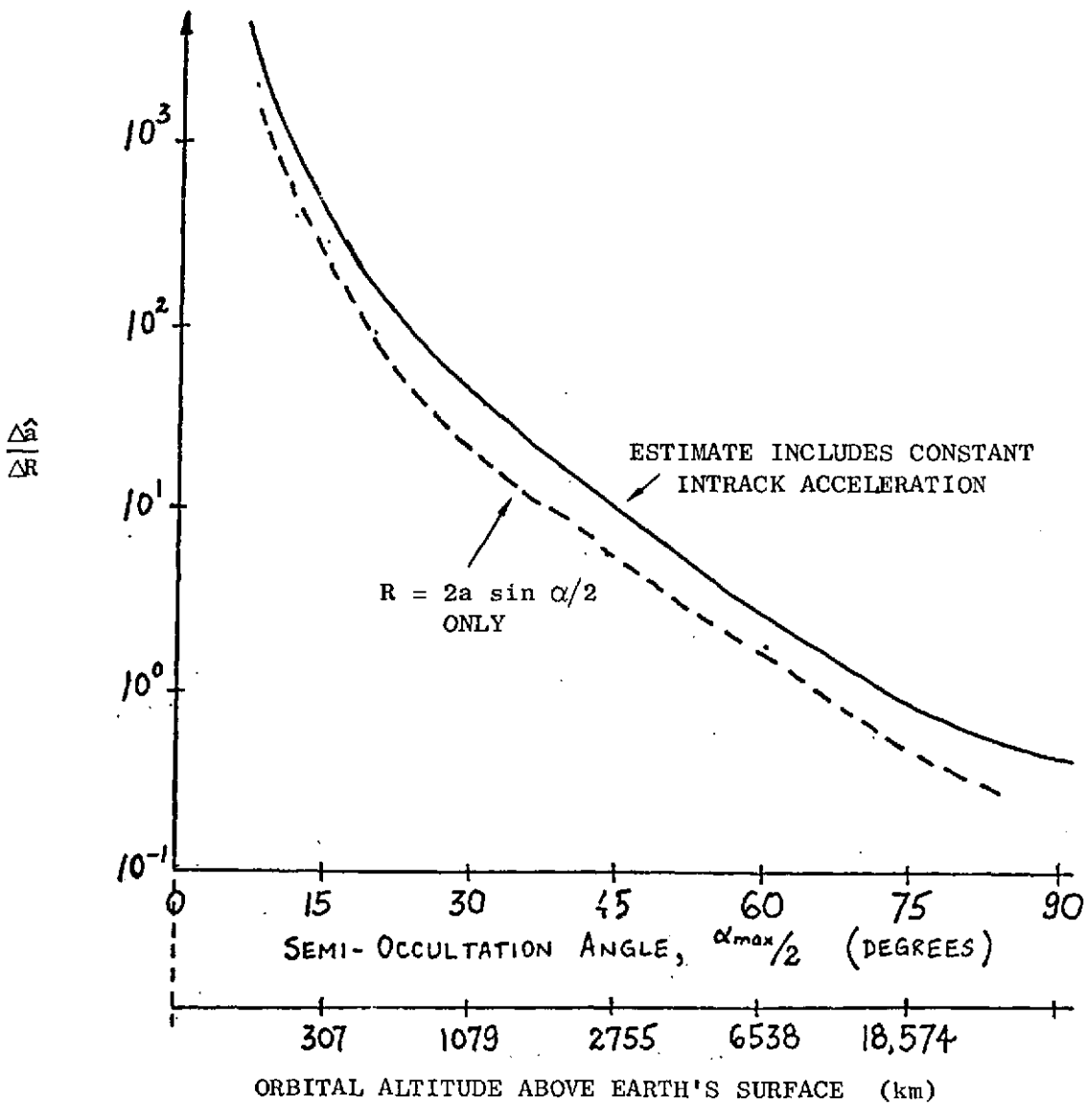

FIG. 7 BIAS IN THE ESTIMATE OF SEMI-MAJOR AXIS DUE TO CONSTANT BIASES IN RANGE MEASUREMENT

random process with standard deviation σ_A of order of magnitude 10^{-11}g and a correlation time τ_A of order of the spin period.

The effect of such a random relative acceleration on the separation α and hence on the estimate of a is summarized in Figure 8.

From Figure 7 we see that it will suffice to reduce the bias ΔR in range measurement to 10 cm, if the orbital altitude exceeds 1000 km.

From Figure 8, if we assume, for example, an altitude of 1000 km and a separation rate of 6×10^{-6} rad/sec $\cong 3°$/day, then using $\sigma_A \cong 10^{-11}$g, $\tau_A = 1$ sec, $\sigma_{\hat{a}}/a \cong 0.3(10^{-7})$.

It should be added that Figure 8 was calibrated for the average fit of a noise-free model to data obtainable with a noisy intrack acceleration. It is for this reason that a slower separation rate $\dot{\alpha}$ would actually increase the error of the estimation. An optimal filtering scheme would not have had this defect.

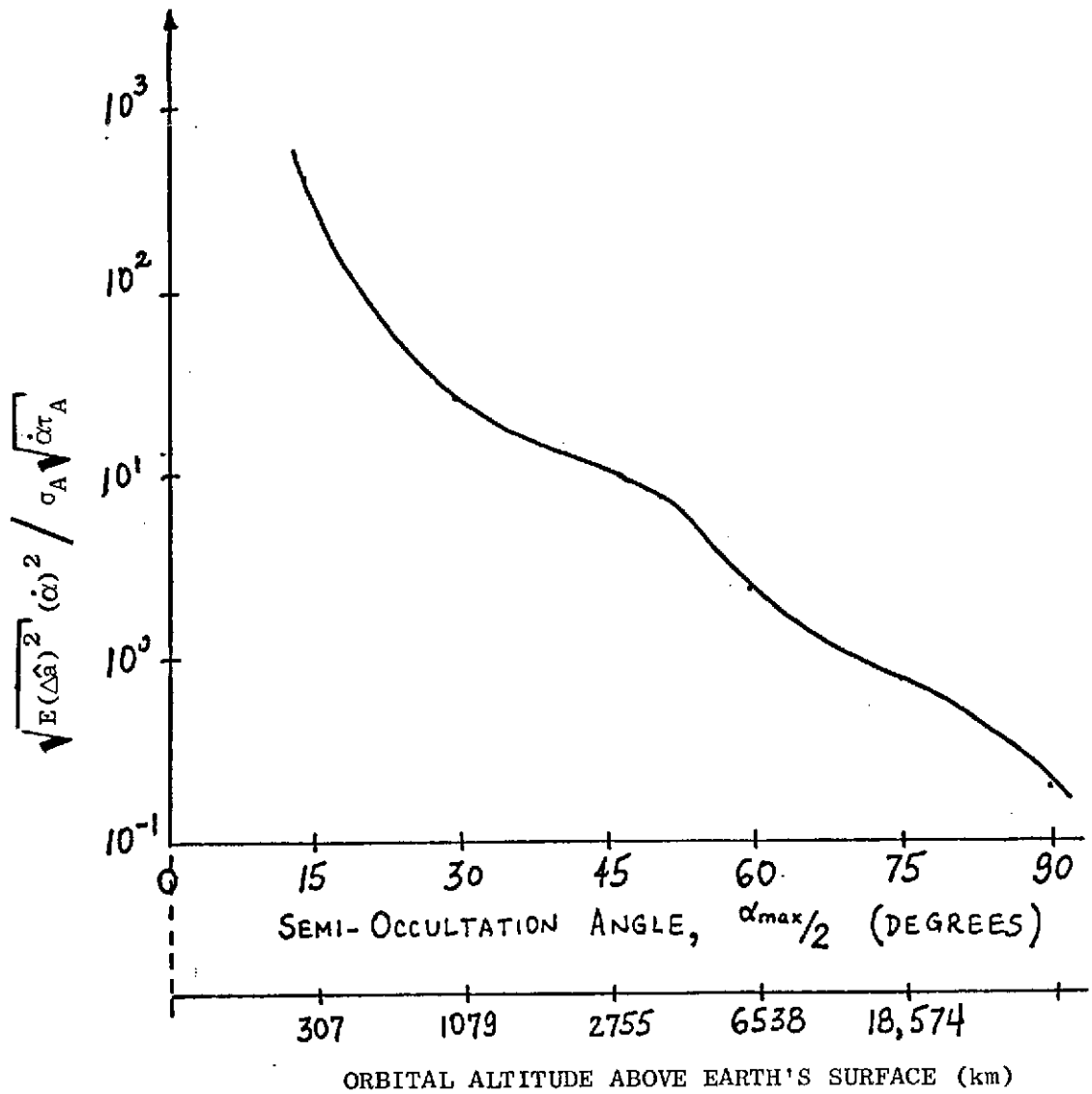

FIG. 8 RMS ERROR IN THE ESTIMATE OF THE SEMI-MAJOR AXIS DUE TO SMALL RANDOM INTRACK ACCELERATION.

REFERENCES

1. Proposal to DEVELOP MINIMUM THRUSTOR CONTROL LAWS AND SELECT ORBITS FOR A GEODESY DRAG-FREE SATELLITE, submitted to the Goddard Space Flight Center of the NASA by Stanford University, Guidance & Control Laboratory of Aeronautics and Astronautics Dept., Jul 1971.

2. Monthly Report to Study to Develop Minimum Thrust Control Laws and Select Orbits for a Geodesy Drag-Free Satellite, Monthly Reports 1 through 9, submitted to Goddard Space Flight Center, Code 551, by Stanford University.

3. Work Statement from Goddard Space Flight Center relative to "Proposal To Develop Minimum Thrustor Control Laws and Select Orbits for a Geodesy Drag-Free Satellite," 1972

4. Dasenbrock, R.R., "Some Higher Order Analyses of Earth and Lunar Orbiters," Ph.D. Dissertation, Dept. Aeronautics and Astronautics, Guidance & Control Lab., Stanford University, Stanford, Calif., 94305, May 1971, SUDAAR No. 424.

5. Morrison, Angus, "Orbit Determination for a Weather Occultation Satellite," Ph.D. Dissertation, Dept. Aeronautics and Astronautics, Guidance & Control Lab., Stanford University, Stanford, Calif., 94305, Fall, 1972.